




ORIGINAL ARTICLE

Anatomical Study of the Common Fox (*Vulpes vulpes*) Thoracic Cavity with CT Scan

Nima Mozaffari¹, Mohsen Abbasi ², Omid Zehtabvar³, Alireza Vajhi⁴, Amir Zakian¹, Yasin Valizadeh¹

¹ Department of Clinical Sciences, Faculty of Veterinary Medicine, Lorestan University, Khorramabad, Iran. ² Department of Basic Sciences, Faculty of Veterinary Medicine, Lorestan University, Khorramabad, Iran. ³ Department of Basic Sciences, Faculty of Veterinary Medicine, University of Tehran, Tehran, Iran. ⁴ Department of Surgery and Radiology, Faculty of Veterinary Medicine, University of Tehran, Tehran, Iran.

ARTICLE INFO

ABSTRACT

Article History:

Received: 16 October 2024

Revised: 17 January 2025

Accepted: 1 February 2025

Keywords:

Common fox
Anatomy
Thoracic cavity
CT scan

This study investigates the thoracic cavity anatomy of the red fox (*Vulpes vulpes*) using computed tomography (CT) and 3D image reconstruction techniques. Four healthy male foxes were scanned, and their thoracic structures, including the heart, lungs, trachea, and bronchi, were analyzed. The findings revealed that the red fox possesses 13 pairs of ribs, with the right lung being more caudally extended compared to the left, contrary to many other species. The heart was positioned between the fifth and tenth ribs, angled to the left of the midline. Both the right and left primary bronchi were similar in length and diameter, a feature also noted in other species, such as guinea pigs and dogs. These results contribute to a more detailed understanding of red fox thoracic anatomy, offering a baseline for comparative studies and aiding future diagnostic procedures. The use of non-invasive CT scans provides valuable insights into the positioning and measurements of thoracic organs without the need for invasive methods, establishing this approach as a reliable and ethical means of studying the anatomy of wildlife and other species.


Introduction

The red fox, scientifically classified as *Vulpes vulpes*, is a member of the phylum Chordata, the class Mammalia, the order Carnivora, and the family Canidae. Among the members of the order Carnivora, the red fox boasts the widest geographical distribution.¹

Old methods, such as dissection, while often more accessible and economically efficient, are considered invasive. Because of this, they may not be suitable for studying valuable species, those in sensitive habitats, or endangered species. Furthermore, they do not accurately depict the shape and relative positioning of structures. Various diagnostic imaging methods, including radiology, computed tomography (CT) scans, and MRI, are non-invasive and well-suited for examining internal structures in their precise anatomical locations.² Radiography and CT scan

imaging techniques provide a standard anatomical view of various body structures in living animals. These methods are considered valuable tools for diagnosing injuries and complications within body organs.³

The advantage of a CT scan lies in its ability to detect and distinguish between various types of soft tissue. This capability is achieved by accurately measuring the amount of X-rays absorbed by different tissues, resulting in excellent image contrast. In a CT scan, tissues and structures are characterized by their "attenuation," which is their ability to block X-rays. In radiology, attenuation is essentially synonymous with "radiopacity." The term "isoattenuating" describes tissues with the same attenuation and, consequently, the same shade of gray on the scan. If a tissue's attenuation or its ability to impede X-rays is lower than that of a reference tissue or the expected level for that

 Corresponding author. Email: abasi.m@lu.ac.ir

© Iranian Veterinary Surgery Association, 2025

<https://doi.org/10.30500/ivsa.2025.483929.1419>



This work is licensed under the Creative Commons Attribution-NonCommercial 4.0 International License. To view a copy of this license, visit <http://creativecommons.org/licenses/by-nc/4.0/>

tissue type, it is termed "hypoattenuating" and appears as a darker shade of gray. Conversely, tissues with higher-than-expected attenuation are described as "hyperattenuating" and appear lighter. The gray levels in CT images can be adjusted to optimize the visibility of organs with different attenuation levels. This process is known as "windowing". Specialized windows tailored to specific tissues are used to examine particular organs or structures. For example, the lung window is particularly useful for assessing lung details.³⁻⁶

In 1993, Smallwood *et al.* conducted a CT scan investigation of the chest, abdominal cavity, and pelvis in dogs and subsequently compiled an atlas based on their findings.⁷ In 2003, Shojaei *et al.* identified and named anatomical structures within CT scan images of a cat's thoracic cavity. Their research data could serve as a valuable reference for future studies on feline thoracic anatomy.⁸ In 2018, Kazemi-Darabadi and colleagues used CT scans to study the anatomy and topography of the lower respiratory tract in the southern white-breasted hedgehog.⁹ In 2005, De Rycke *et al.* examined the anatomical sections of the thoracic cavity in adult German Shepherd dogs, comparing them with CT scan images. Through this comparison, they introduced CT scanning as a suitable method for diagnostic chest imaging.¹⁰ In 1998, Samii *et al.* investigated the normal cross-sectional anatomy of the thoracic and abdominal cavities in cats, using two domestic short-haired cats for their study.¹¹ In 2014, Zahtabvar *et al.* studied the anatomical structure of the lower respiratory system in the European pond turtle.¹² In 2023, Zehtabvar *et al.* conducted a research project to provide detailed topographic information about the trachea, bronchi, lungs, and heart within the thoracic cavity of Guinea pigs. The study also examined the features of these structures, their proximity to other organs, and performed comparative anatomical analyses using CT scan images of live specimens.¹³

The purpose of this study is to provide a detailed anatomical understanding of the thoracic cavity of the red fox (*Vulpes vulpes*) using non-invasive CT imaging techniques. This research aims to establish baseline anatomical data that can serve as a reference for comparative anatomical studies and support diagnostic and therapeutic interventions in wildlife medicine.

Materials and Methods

Ethical Considerations

The procedures of this work were approved by the University Ethical Committee and filed under LU.ECRA.2019.22 code.

Animals

Four healthy male foxes with a mean weight of 2.5 kg were used in this study. The foxes were kept in the

wildlife rehabilitation center of Pardisan in Tehran. To generate CT scan images, each fox was physically restrained, and then a catheter was placed in the cephalic vein. Premedication was administered with an intravenous injection of 20 µg/kg dexmedetomidine (Exir Pharmaceutical Co., Iran). Anesthesia was induced by intravenous injection of 4 mg/kg ketamine (Bremer Pharma Co., Germany). Then, the foxes were transferred to a diagnostic imaging center at the Veterinary Teaching Hospital of the University of Tehran. After completing the imaging process and allowing the foxes to recover from anesthesia, a 0.9% normal saline solution was administered intravenously to all foxes at a rate of 10 ml/kg per hour. Throughout the CT scan and recovery period, the foxes were maintained at a consistent room temperature (23-25 °C).¹⁴

Computed Tomographic (CT Scan) Examination and Morphometric Evaluation

The foxes were positioned in ventral recumbency under general anesthesia on the CT scan machine table. CT images of the entire thoracic region were obtained using a helical scanner (Somatom Spirit Series Dual Slice CT Scanner, Siemens, Germany). The technical CT parameters were as follows: rotation time, 1s; slice thickness, 1 mm; Reconstruction interval, 2 mm; pitch, 1; X-ray tube potential, 130 kV; and X-ray tube current, 108 mA. Appropriate window levels (WL) and window widths (WW) were selected for analysis in each section. The bone and lung windows were used to view the images. Three-dimensional reconstruction was performed using RadiAnt DICOM Viewer software for morphometric measurements.

Statistical Analysis

The measurement results were statistically analyzed using a paired t-test in SPSS software. Additional statistical analysis was conducted with MedCalc statistical software (version 20.104, MedCalc Software Ltd., Ostend, Belgium), with the significance level set at $p < 0.05$. The parameters measured, along with their descriptions, are presented in Table 1.

Results

In this study, the location, anatomy, and measurements of the main organs in the thorax were determined using CT scans and 3D image reconstruction. Each fox had 132 CT scan sections, with images displayed in order from the cranial end of the thoracic region. The distance between consecutive images was 2 mm. The transverse plane is preferred for most general assessments, particularly in chest and abdominal imaging. In this study, the nomenclature and delineation of organ locations were primarily performed in the

transverse plane, while the sagittal and coronal planes were used to provide a comprehensive overview of organ location and positioning.

Thorax

The thorax of the common fox consists of 13 pairs of ribs. The nine cranial ribs are attached directly to the sternum, while the last ribs (the 13th pair) are floating. In the transverse CT images, the most cranial part of the diaphragm was scanned immediately after the heart ended, at the level of the 12th rib, and beyond.

Trachea and bronchi

The thoracic trachea begins at the thoracic inlet and

continues to the tracheal bifurcation. It extends from the first rib to the sixth rib, or in some cases, to the sixth intercostal space. The tracheal bifurcation is located at the caudal edge of the sixth rib, just before the start of the seventh rib (Figures 1 and 2). The thoracic trachea is inclined to the right side of the midline, and its length for the studied cases is listed in Table 2. The diameter of the tracheal rings generally decreases as they approach the bifurcation. Both the left and right bronchus extended from the sixth intercostal space to the eighth rib. The bronchi entered the lungs at the level of the eighth rib (Figure 3). Also, the main bronchi incline dorsally after the tracheal bifurcation. The variance in the length and diameter of the right and left primary bronchus did not reach statistical significance.

Table 1. Description of the measured morphometric parameters.

Parameter	Unit	Description
Diameter of the left primary bronchus	mm	The diameter of the bronchus was measured immediately after branching from the trachea.
Diameter of the right primary bronchus	mm	The diameter of the bronchus was measured immediately after branching from the trachea.
Long axis of the heart	cm	In the sagittal plane long axis of the heart was measured from the ventral border of the tracheal bifurcation to the cardiac apex.
Short axis of the heart	cm	In the midsagittal plane of the caudal vena cava, this parameter was measured along the atrioventricular valves.
Tracheal height at thoracic inlet	mm	To measure this parameter, tracheal height was measured at the entrance to the thorax near the first thoracic vertebrae.
Tracheal width at thoracic inlet	mm	To measure this parameter, tracheal width was measured at the entrance to the thorax near the first thoracic vertebrae.
Right lung length	cm	In the 3D reconstructed CT scan images with pulmonary pattern, the maximal length was measured from apex to the most caudal point of the lung diaphragmatic border.
Left lung length	cm	In the 3D reconstructed CT scan images with pulmonary pattern, the maximal length was measured from apex to the most caudal point of the lung diaphragmatic border.
Right lung width	cm	In the 3D reconstructed CT scan images with pulmonary pattern, the maximal width was measured.
Left lung width	cm	In the 3D reconstructed CT scan images with pulmonary pattern, the maximal width was measured.
Right lung height	cm	In the 3D reconstructed CT scan images with pulmonary pattern, the maximal height was measured.
Left lung height	cm	In the 3D reconstructed CT scan images with pulmonary pattern, the maximal height was measured.
Right bronchus length	cm	It was measured from the tracheal bifurcation to the entry of bronchus into the lung, In the 3D reconstructed CT scan images with pulmonary pattern.
Left bronchus length	cm	It was measured from the tracheal bifurcation to the entry of bronchus into the lung, In the 3D reconstructed CT scan images with pulmonary pattern.
Right lung volume	cm ³	This parameter was measured using MMWP VE40A software, Hounsfield unit (HU) was adjusted -700 to -600 (HU for lung).
Left lung volume	cm ³	This parameter was measured using MMWP VE40A software, Hounsfield unit (HU) was adjusted -700 to -600 (HU for lung).
Heart volume	cm ³	This parameter was measured using MMWP VE40A software, Hounsfield unit (HU) was adjusted -120 to 60 (HU for oil and soft tissues).
Thoracic cavity volume	cm ³	This parameter was measured using MMWP VE40A software, Hounsfield unit (HU) was adjusted -700 to 60 (HU for oil, lung and soft tissues).
Thoracic tracheal length	cm	It was measured from the entry of trachea into the thorax to the tracheal bifurcation, In the 3D reconstructed CT scan images with pulmonary pattern.
Angle of trachea to spine	°	The angle between the tangent to the dorsal edge of the thoracic trachea and the tangent to the ventral edge of the thoracic part of the vertebral column.
Vertebral heart score	number	The long and short axis dimensions were added, transposed onto the vertebral column and recorded as the number of vertebrae starting at the cranial edge of the 4th thoracic vertebra. The given distance along the vertebral column to the caudal point was estimated as the number of vertebrae resulting in a vertebral heart score.

Table 2. Morphometric studies results.

parameter	Units	Mean \pm SD
Diameter of the left primary bronchus	mm	6.29 \pm 0.32a
Diameter of the right primary bronchus	mm	6.48 \pm 0.28a
Long axis of the heart	cm	5.22 \pm 0.25
Short axis of the heart	cm	3.31 \pm 0.21
Tracheal height at thoracic inlet	mm	7.42 \pm 0.26
Tracheal width at thoracic inlet	mm	6.18 \pm 0.44
Right Lung length	cm	12.64 \pm 0.12b
Left Lung length	cm	15.31 \pm 0.28b'
Right Lung width	cm	4.07 \pm 0.58c
Left Lung width	cm	3.92 \pm 0.58c
Right Lung height	cm	5.24 \pm 0.13d
Left Lung height	cm	5.34 \pm 0.22d
Right Bronchus length	cm	2.21 \pm 0.32e
Left Bronchus length	cm	2.33 \pm 0.11e
Right Lung volume	cm ³	11.25 \pm 0.58f
Left Lung volume	cm ³	13.11 \pm 0.31f'
Heart volume	cm ³	9.36 \pm 0.58
Thoracic cavity volume	cm ³	40.36 \pm 0.58
Thoracic tracheal length	cm	5.19 \pm 0.58
Angle of trachea to spine	°	6.68 \pm 0.72
Vertebral heart score	number	8.61 \pm 0.37

A Latin letter is considered for each parameter. Identical letters mean non-significance and letters with a sign (') mean a significant difference.

Table 3. The location of organs in the thoracic cavity.

Organ \ Rib no	1	2	3	4	5	6	7	8	9	10	11	12	13	Description
Thoracic trachea														From the 1st to the 6th rib to tracheal bifurcation
Right bronchus														From the 6th to the 8th rib
Left bronchus														From the 6th to the 8th rib
Right lung														From the beginning of the 2nd rib or the end of the first rib to the 13th rib
Left lung														From the first rib to the 12th rib
Heart														From the 5th intercostal space to the 10th rib or the tenth intercostal space

Lungs

In all foxes, the left lung was positioned slightly more cranially than the right lung, and the cranial lobe of the left lung started from the first rib at the beginning of the thoracic cavity. The left lung extended in length up to the twelfth rib. The right lung began at the first intercostal space or the second rib and extended to the thirteenth rib (Figure 3). The length, width, and height of the lungs were measured in all four foxes by reconstructing 3D CT scan images. According to the measurements, the length and volume of the left lung were significantly greater than those of the right lung, though the difference in width

between the right and left lungs did not reach statistical significance. The combined volume of the right and left lungs accounted for 60.35% of the total volume of the chest cavity.

Cardiovascular

The heart of the common fox was egg-shaped in the sagittal view, with its longitudinal axis forming an angle of approximately 45 degrees to the sternum. The heart originated at the fifth intercostal space, extended to the tenth rib, and was inclined toward the left side of the chest (Figure 3). In the axial plane of CT images, the right atrium

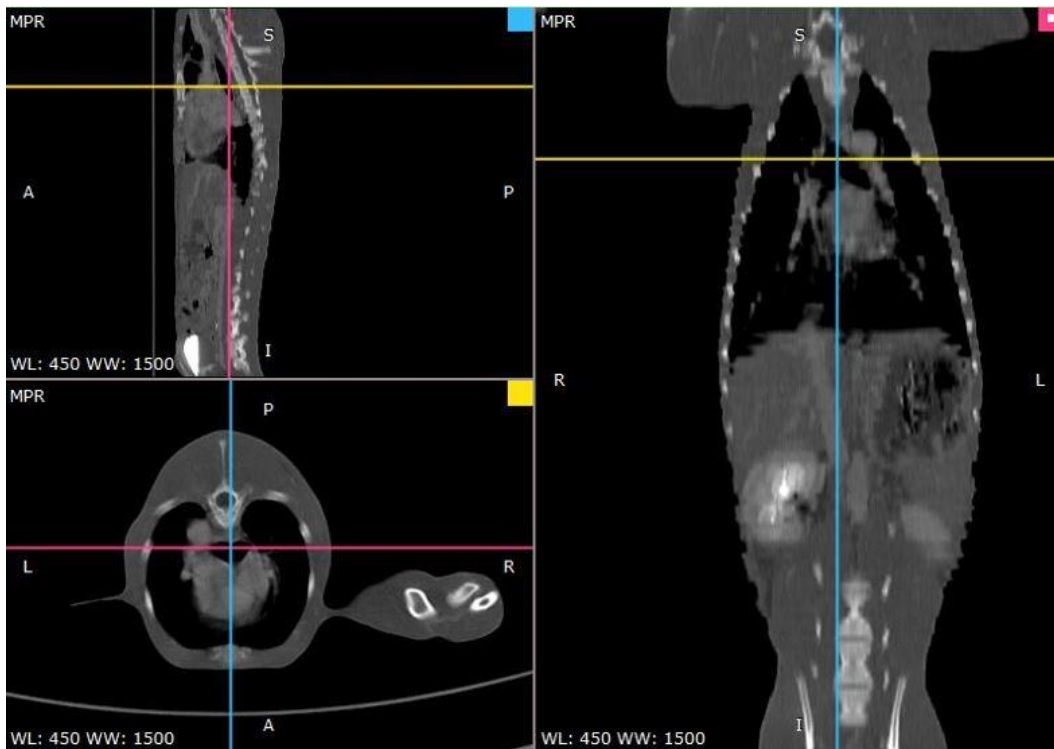


Figure 1. Tracheal bifurcation in coronal view (right), sagittal view (top left), and axial view (down left).

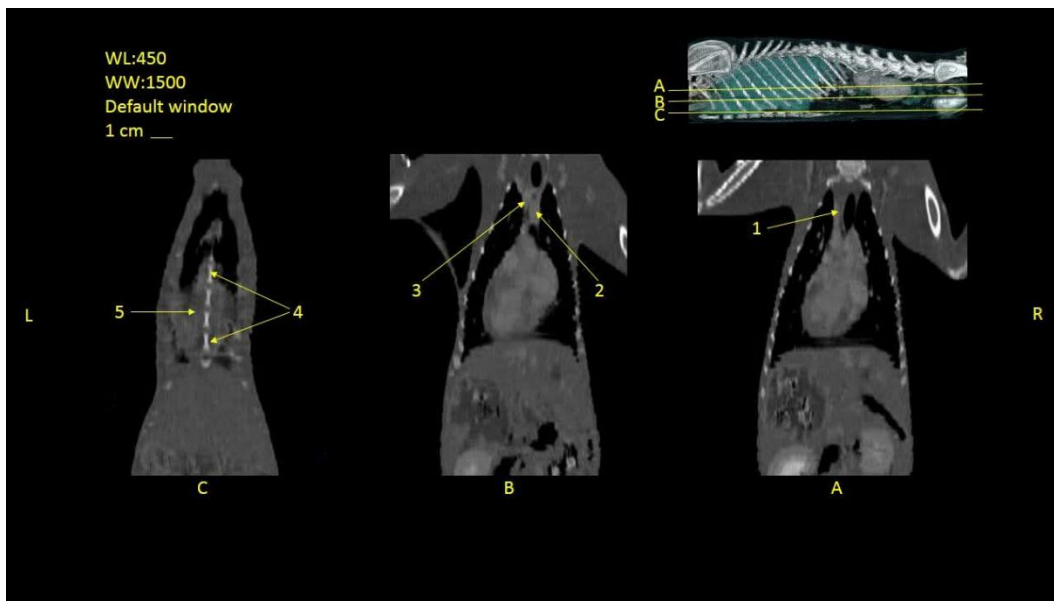


Figure 2. Coronal view of thorax (default window). The three-dimensional image above shows the section sites have been marked. 1. Left subclavian artery, 2. Brachiocephalic artery, 3. Left common carotid artery, 4. Sternum, 5. Heart.

was observed as the most cranial section of the heart. The heart comprised 23.19% of the total volume of the chest cavity. The primary vessels visible in the thoracic cavity, in the transverse view ranging from the third to fourth ribs (cranial to caudal), were the left subclavian artery, the left common carotid artery, and the brachiocephalic artery. The left subclavian artery and the left common carotid artery were located on the left side of the midline, while the brachiocephalic artery was positioned on the right, arising from the aortic arch. All three arteries were identified and named in the sagittal, coronal, and axial views (Figures 2, 3, and 4).

At the cranial edge of the sixth rib, the ascending aorta, descending aorta, and pulmonary arteries were visible in

a single section (Figures 3 and 5). Another vessel observed in the CT images was the caudal vena cava, located in the caudal part of the chest and on its right side. Table 2 provides a summary of all measurements while Table 3 displays the organ locations within the thoracic cavity.

Discussion

This study investigated the anatomical position and measurement of the organs in the thoracic cavity of the common fox. Diagnosing thoracic cavity organ diseases and abnormalities requires a thorough understanding of their normal anatomy. To successfully carry out treatments, including surgery, a thorough knowledge of

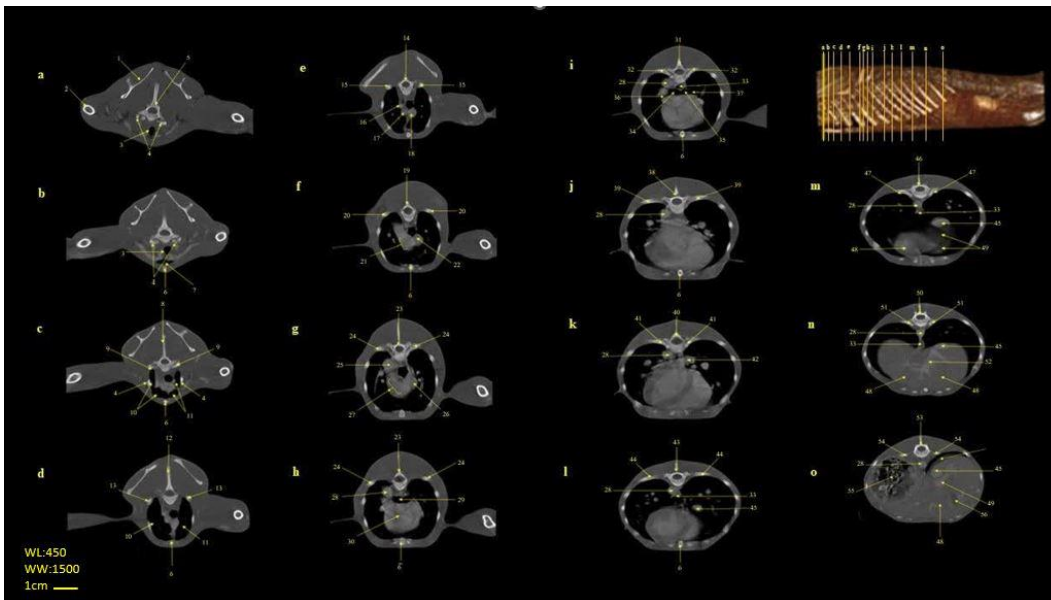


Figure 3. Transverse CT scan images of the thorax (Bone window), Common Fox, in 3D image the section sites have been marked. 1. Scapula, 2. Humerus, 3. Trachea, 4. 1st rib, 5. Thoracic vertebra (T1), 6. Sternum, 7. Cranial lobe of left lung, 8. Thoracic vertebra (T2), 9. 2nd rib, 10. Left lung, 11. Right lung, 12. Thoracic vertebra (T3), 13. 3rd rib, 14. Thoracic vertebra (T4), 15. 4th rib, 16. Left subclavian, 17. Left common carotid artery, 18. Brachiocephalic artery, 19. Thoracic vertebra (T5), 20. 5th rib, 21. Aortic arch, 22. Cranial vena cava, 23. Thoracic vertebra (T6), 24. 6th rib, 25. Descending aorta, 26. Ascending aorta, 27. Pulmonary artery, 28. Aorta, 29. Tracheal bifurcation, 30. Heart, 31. Thoracic vertebra (T7), 32. 7th rib, 33. Esophagus, 34. Left bronchus, 35. Right bronchus, 36. Entrance of the left bronchus to the left lung, 37. Entrance of the right bronchus to the right lung, 38. Thoracic vertebra (T8), 39. 8th rib, 40. Thoracic vertebra (T9), 41. 9th rib, 42. Right pulmonary artery, 43. Thoracic vertebra (T10), 44. 10th rib, 45. Caudal vena cava, 46. Thoracic vertebra (T11), 47. 11th rib, 48. Liver, 49. Diaphragm, 50. Thoracic vertebra (T12), 51. 12th rib, 52. Portal vein, 53. Thoracic vertebra (T13), 54. 13th rib, 55. Stomach, 56. Gall bladder.

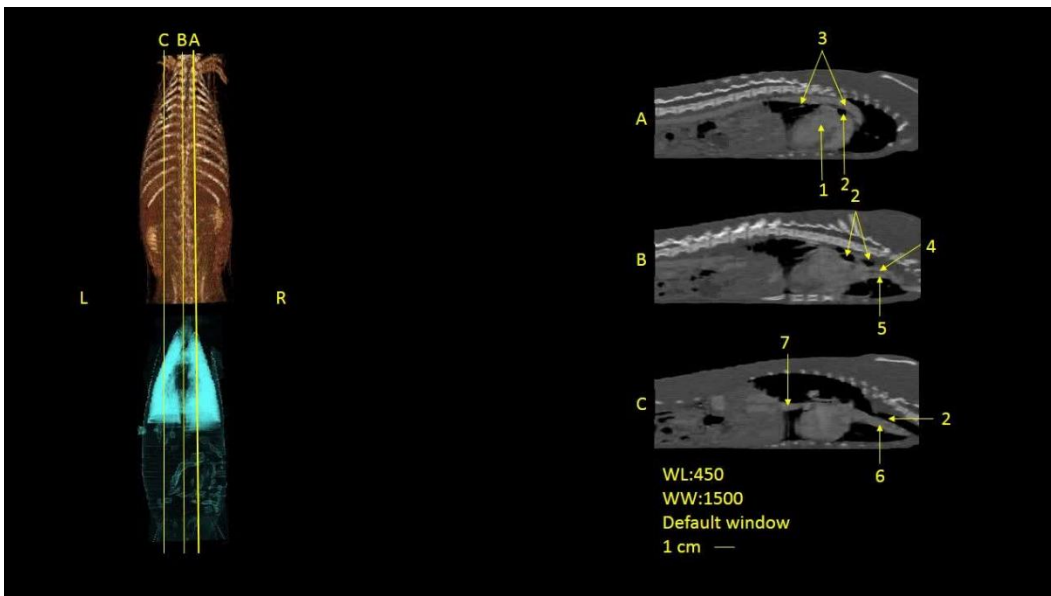


Figure 4. Sagittal view of thorax (default window). The three-dimensional image on left shows the section sites that have been marked. 1. Heart, 2. Trachea, 3. Aorta, 4. Left subclavian artery, 5. Left common carotid artery, 6. Brachiocephalic artery, 7. Caudal vena cava.

the precise locations of vital organs is indispensable. The use of non-invasive CT scans is an effective and ethical approach to gather this anatomical information. The results of this study can serve as a valuable reference for future research. Researchers studying red foxes or related species may refer to these findings when conducting their investigations into thoracic cavity anatomy or related topics.

In 1993, the study conducted by Smallwood and colleagues led to the preparation of an atlas of CT scan images of two collared beagle dogs. In this study, the

major vessels in the thoracic cavity were identified and named. The tracheal bifurcation was found to be located at the level of the fifth rib and the fifth thoracic vertebra. Additionally, similar to our study on foxes, the left lung was found to occupy a more cranial position than the right lung.⁷ In 1998, Samii *et al.* investigated the normal anatomy of the thoracic and abdominal cavities in cats using transverse sections. The study utilized two domestic short-haired cats, with CT scan images taken from the beginning of the manubrium to the hip joint. Following imaging, the cats were euthanized and

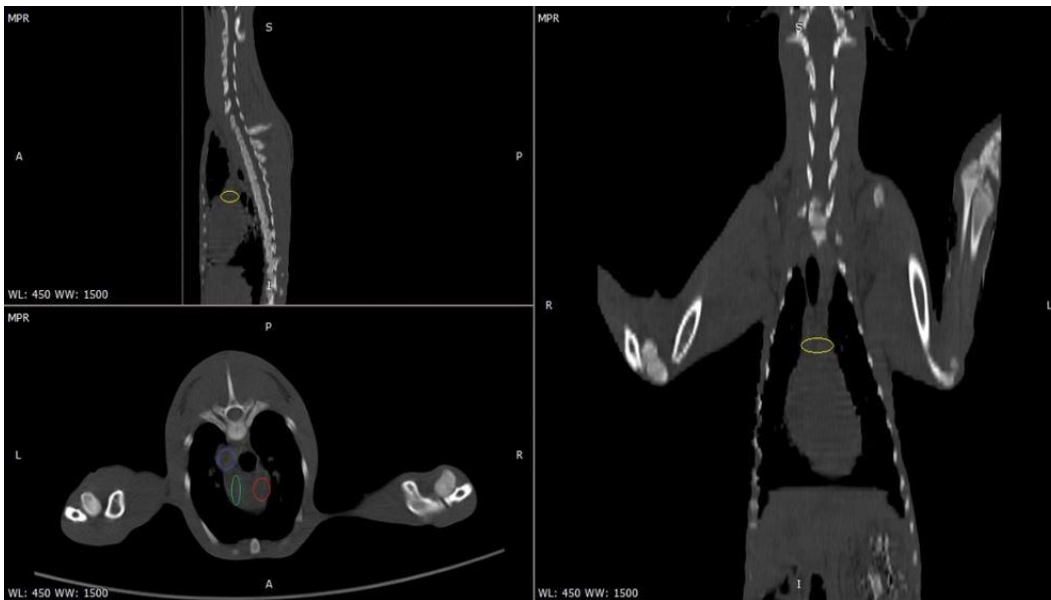


Figure 5. The location of the ascending aorta, descending aorta, and pulmonary artery in coronal view (right side) and sagittal view (top left) which are marked with yellow color. In the axial view (lower left), the descending aorta (blue), ascending aorta (red), and pulmonary artery (green) are marked.

positioned identically to the CT scan images. The goal of Samii *et al.*'s study was to create an atlas of cross-sectional images of the thoracic and abdominal regions in cats to aid in the interpretation of these images. In contrast with our study, Samii *et al.* did not measure the sizes of major organs in the thoracic cavity, such as the lungs and heart. Furthermore, the precise locations of the organs in the thoracic cavity were not specified, as the study mainly focused on the correlation between cadaver cross-sections and CT scan images.¹¹ In 2005, De Rycke *et al.* conducted a study on the cross-sectional anatomy of the thorax in healthy dogs. They used four healthy adult German Shepherd dogs for this study. Following the CT scan, one of the dogs was euthanized for a detailed examination of its cross-sectional anatomy. The study observed a correlation between the CT scan images and the transverse sections obtained through dissection. In their study, the tracheal bifurcation was found to be at the same level as the sixth rib and the sixth thoracic vertebra, a finding consistent with the results of our study on the red fox. Additionally, the left lung in dogs was positioned more cranially than the right lung, similar to the fox. The caudal lobe of the right lung extended further caudally than that of the left lung, demonstrating a similarity between the common fox and the dog in this regard. The heart in dogs was located between the fourth and eighth ribs, while in the fox, it extended from the fifth intercostal space to the ninth intercostal space.¹⁰ The main vessels in the thoracic cavity, including the ascending aorta, descending aorta, caudal vena cava, pulmonary artery, brachiocephalic artery, common carotid artery, and subclavian artery, were identified in the CT scans of the thoracic cavity of beagle dogs, similar to our study on common foxes.^{7,10} In 2024, Ibrahim *et al.* provided a comprehensive characterization of the thorax of Shirazi

cats by comparing the relevant soft tissue and bone windows of CT and magnetic resonance imaging (MRI) with cross-sectional, sagittal, and coronal anatomical perspectives. The mediastinal contents and their relationship with the lungs and diaphragm were detailed in coronal-sectional anatomy and CT slices. The thoracic inlet was described as being bounded dorsally by the 1st thoracic vertebra, laterally by the 1st rib, and ventrally by the 1st sternebra. The cranial lobe of the right lung began to appear at the level of the 2nd intercostal space, with both cranial lobes of the right and left lungs visible at the level of the 3rd rib. In contrast to the lung position in the fox, the right lung in cats was positioned slightly more cranially than the left lung. While the caudal lobe of the right lung terminated, the caudal lobe of the left lung extended further caudally, reaching the 9th intercostal space. The heart occupied most of the middle mediastinum, with the cranial part of its base located just caudal to the 4th rib, while its apex extended caudally to approximately the middle of the 7th intercostal space. In cats, the trachea bifurcated at the level of the 5th rib, whereas in foxes, it occurred at the 6th intercostal space. At the 6th thoracic vertebra, the right and left bronchi entered their respective lungs, whereas in foxes, the bronchi entered the lungs at the level of the 8th rib. The distribution of thoracic vessels was clearly visible on cross-sectional and coronal contrast-enhanced CT scans.¹⁵ In 2018, Kazemi Darabadi *et al.* investigated the anatomy and CT scan of the lower respiratory system in the southern white-breasted hedgehog. Anatomical studies revealed that the left lung lacks lobulation and consists of a single part, whereas the right lung is divided into four lobes. The lungs extend from the second rib to the last rib. The right lung demonstrated a greater volume than the left lung, which contrasts with our observations

in the common fox. Unlike the fox, which has bronchi of the same size, the southern white-breasted hedgehog exhibited a shorter right bronchus compared to its left bronchus. The heart in the southern white-breasted hedgehog was located between the second and seventh intercostal spaces, whereas in the red fox, it spanned from the fifth intercostal space to the tenth rib.⁹ In 2023, Zehtabvar *et al.* demonstrated that the heart in the guinea pig was not inclined to the left but was almost on the midline, contrary to what is observed in the fox. Differences between these two species in the number of ribs were noted. The thorax of the adult English Guinea pig exhibited 14 pairs of ribs, with the last 5 classified as floating ribs. In contrast, the fox displayed 13 pairs of ribs, with the final ones also identified as floating. Additionally, it was observed that, unlike foxes, the lungs of English Guinea pigs are equal in size. No significant difference was found in the length and diameter of the right and left primary bronchi in either species. Finally, the angle of the trachea to the spine was greater in the Guinea pig compared to the fox.¹² Unlike the findings regarding lung volume in common foxes, Müllhaupt *et al.* observed in their examination of New Zealand white rabbits that the right lung volume in rabbits was significantly greater than the left lung's volume.¹⁶ The location of the tracheal bifurcation was found to be at the sixth rib, highlighting a similarity between the red fox and the German Shepherd breeds and Shirazi Cats in terms of the starting point of the bronchi.^{10,15} The location of the heart differed slightly between cats, dogs, and foxes. In foxes, the heart was located between the 5th and 10th intercostal spaces, whereas in cats and dogs, it was situated more cranially, between the 4th and 8th ribs.^{7,10,15} Another similarity between dogs and the common fox was that the left lung was more cranial than the right lung and started at the first rib.^{7,10} Another feature common to foxes and other examined species was the rightward positioning of the trachea and the leftward positioning of the heart relative to the midline. The shape of the heart varied across species: in dogs, it was egg-shaped; in ruminants, it was conical with a sharp tip; and in rabbits and rodents, it had a drawn, sharp tip.^{9,10,16}

Understanding the thoracic anatomy of the red fox has direct implications for veterinary diagnostics, surgical planning, and wildlife conservation. For instance, the cranial positioning of the left lung and the heart's inclination to the left could influence thoracic imaging interpretations and interventions. Additionally, the data provide a baseline for identifying pathological changes in foxes and related species.

The observed anatomical adaptations may also reflect ecological and behavioral factors unique to the red fox. For example, the positioning of the lungs and heart could enhance respiratory efficiency and cardiovascular

performance, supporting the fox's agility and endurance in its natural habitat.

This study underscores the value of advanced imaging techniques in wildlife research. By comparing the red fox's thoracic anatomy with other species, the findings enrich our understanding of mammalian anatomical diversity. Moreover, the ethical and non-invasive nature of CT imaging sets a standard for future anatomical studies in wildlife and domestic animals.

In conclusion, this study provides a comprehensive anatomical analysis of the thoracic cavity in the red fox (*Vulpes vulpes*) using advanced CT imaging. Key findings include the unique positioning of the heart, lungs, trachea, and bronchi, along with precise morphometric data on these structures. The discovery that the left lung extends more cranially than the right and the heart's inclination to the left are among the notable distinctions of red fox anatomy compared to other species such as dogs, cats, guinea pigs, and hedgehogs. The use of non-invasive CT imaging proved to be a reliable and ethical method for obtaining detailed anatomical information without harm to the animals. These results offer a valuable baseline for future comparative studies and enhance the understanding of thoracic anatomy, which is critical for wildlife conservation efforts, veterinary diagnostics, and treatment planning. Ultimately, this research highlights the importance of employing advanced imaging techniques to gain insights into the complex anatomy of wildlife species, contributing significantly to veterinary science and comparative anatomy studies.

Conflict of Interest

There is no conflict of interests to declare.

References

1. Sillero-Zubiri C, Hoffmann M, Macdonald DW, eds. Canids: foxes, wolves, jackals, and dogs: status survey and conservation action plan. IUCN, Gland, Switzerland, 2004.
2. Sisson S. The anatomy of the domestic animals. WB Saunders Company, 1914.
3. Thrall DE. Textbook of veterinary diagnostic radiology-e-book, Elsevier Health Sciences, 2012.
4. Burk RL, Ackerman N. Small animal radiology and ultrasonography: A diagnostic atlas and text. 1996.
5. Kealy JK, McAllister H, Graham JP. Diagnostic radiology and ultrasonography of the dog and cat. Elsevier Health Sciences; 2010.
6. Rowlands JA. The physics of computed radiography. *Physics in Medicine and Biology*. 2002; 47(23): R123-166. doi: 10.1088/0031-9155/47/23/201
7. Smallwood JE, George TF. Anatomic atlas for computed tomography in the mesocephalic dog: thorax and cranial abdomen. *Veterinary Radiology and Ultrasound*. 1993; 34(2): 65-84. doi: 10.1111/j.1740-8261.1993.tb01510.x
8. Shojaei B, Rostami A, Vajhi A, Shafaei M. Computed tomographic anatomy of the thoracic region of the cat. *Veterinarski Arhiv*. 2003; 73(5): 261-270.
9. Kazemi-Darabadi S, Akbari G, Ebrahimi E, Zangisheh M. Computed tomographic anatomy and topography of the

- lower respiratory system of the southern white-breasted hedgehog (*Erinaceus concolor*). *Iranian Journal of Veterinary Surgery*. 2018; 13(2): 26-33. doi: 10.22034/ivsa.2018.137920.1150
10. De Rycke LM, Gielen IM, Simoens PJ, van Bree H. Computed tomography and cross-sectional anatomy of the thorax in clinically normal dogs. *American Journal of Veterinary Research*. 2005; 66(3): 512-524. doi: 10.2460/ajvr.2005.66.512
 11. Samii VF, Biller DS, Koblik PD. Normal cross-sectional anatomy of the feline thorax and abdomen: comparison of computed tomography and cadaver anatomy. *Veterinary Radiology and Ultrasound*. 1998; 39(6): 504-511. doi: 10.1111/j.1740-8261.1998.tb01640.x
 12. Zehtabvar O, Masoudifard M, Rostami A, Akbarein H, Sereshke AH, Khanamooeiashi M, Borgheie F. CT anatomy of the lungs, bronchi and trachea in the mature Guinea pig (*Cavia porcellus*). *Veterinary Medicine and Science*. 2023; 9(3): 1179-1193. doi: 10.1002/vms3.1131
 13. Zehtabvar O, Tootian Z, Vajhi A, Shojaei B, Rostami A, Davudypoor S, Sadeghinezhad J, Ghaffari H, Memarian I. Computed tomographic anatomy and topography of the lower respiratory system of the European pond turtle (*Emys orbicularis*). *Iranian Journal of Veterinary Surgery*. 2014; 9(2): 9-16.
 14. Lord J, Miller EA. Natural history and medical management of canids: emphasis on coyotes and foxes. *Medical Management of Wildlife Species: A Guide for Practitioners*. 2019: 313-325. doi: 10.1002/9781119036708
 15. Ibrahim A, Rashwan A, El Sharaby A, Abumandour M, Nomir A. Thoracic cavity of the Shirazi cats: New insights using computed tomography and magnetic resonance imaging. *Anatomia, Histologia, Embryologia*. 2024; 53(1): e13005. doi: 10.1111/ahe.13005
 16. Müllhaupt D, Wenger S, Kircher P, Pfammatter N, Hatt JM, Ohlerth S. Computed tomography of the thorax in rabbits: a prospective study in ten clinically healthy New Zealand White rabbits. *Acta Veterinaria Scandinavica*. 2017; 59: 1-9. doi: 10.1186/s13028-017-0340-x